Available online at www.sciencedirect.com
SCIENCE DIRECT
Bioorganic & Medicinal Chemistry 14 (2006) 5503–5509
Bioorganic & Medicinal Chemistry

Improving anti-trypanosomal activity of 3-aminoquinoxaline-2-carbonitrile N^1,N^4-dioxide derivatives by complexation with vanadium

Carolina Urquiola,[a] Marisol Vieites,[a] Gabriela Aguirre,[b] Adoración Marín,[c] Beatriz Solano,[c] Gabriel Arrambide,[a] Pabla Noblía,[a] María Laura Lavaggi,[b] María H. Torre,[a] Mercedes González,[b] Antonio Monge,[c] Dinorah Gambino[a,*] and Hugo Cerecetto[b,*]

[a]*Cátedra de Química Inorgánica, DEC, Facultad de Química, Universidad de la República, Montevideo, Uruguay*
[b]*Departamento de Química Orgánica, Facultad de Química—Facultad de Ciencias, Universidad de la República, Montevideo, Uruguay*
[c]*Unidad en I + D de Medicamentos, CIFA, Universidad de Navarra, 31080 Pamplona, Spain*

Received 30 March 2006; revised 21 April 2006; accepted 24 April 2006
Available online 18 May 2006

Abstract—New vanadium complexes of the type $[V^{IV}O(L)_2]$, where L are 3-aminoquinoxaline-2-carbonitrile N^1,N^4-dioxide derivatives, were prepared as an effort to obtain new anti-trypanosomal agents improving the bioactivity of the free ligands. Complexation to vanadium of the quinoxaline ligands leads to excellent antiprotozoal activity, similar to that of the reference drugs nifurtimox and benznidazole and in all cases higher than that of the corresponding free ligands. In addition, it is for the first time that the V(^{IV})O–quinoxaline complexes are reported as a family of anti-*Trypanosoma cruzi* agents. Finally, the anti-trypanosomal activity of these vanadium complexes could be explained on the basis of their lipophilicity and the electronic characteristics of the quinoxaline substituents.

1. Introduction

Chagas' disease or American trypanosomiasis is an important health problem that affects around twenty million people in Central and South America. Two to three million individuals develop the typical symptoms of this disease that results in 50,000 yearly deaths.[1,2] The causative agent of this disease is the hemoflagellate protozoan *Trypanosoma cruzi* (*T. cruzi*), which is transmitted to humans and other mammals, in rural areas, by reduviid bugs such as *Rhodnius prolixus* and *Triatoma infestans*.[3] Current pharmacological treatment has been based on benznidazole (Bnz, a nitroimidazole derivative) and nifurtimox (Nfx, a nitrofuran derivative), compounds that cause significant side effects and show poor clinical efficacy.[4–6]

These two drugs are effective against the circulating form of the parasite (trypomastigote) during the acute phase of the disease, but not during the chronic stage.

Several types of compounds have been described as anti-*T. cruzi* agents acting in different biological targets.[7] May be trypanothione reductase (TR) is one of the most thoroughly studied enzymes of the trypanothione redox metabolism, it is a key enzyme of the parasite antioxidant defence system, and it does not occur in the mammalian host.[8] Rational drug design approaches on TR led to the discovery of phenothiazines and other tricyclic drugs (**1** and **2**, Chart 1) as specific competitive inhibitors of the parasite enzyme with low micromolar inhibitor constants without inhibition of the host glutation reductase (GR).[9–11] Some quinoxaline derivatives developed by us[12–14] resembled, by the planar structure and by the kind of substituents, the skeleton of these inhibitors. Consequently, 33 quinoxalines were carefully

Keywords: Anti-trypanosomal activity; Quinoxaline N^1,N^4-Dioxide; Vanadium; *N*,*O* Ligands.
* Corresponding authors. Tel.: +598 25258618; fax: +598 25250749 (H.C.); tel.: +598 29249739; fax: +598 29241906 (D.G.); e-mail addresses: dgambino@fq.edu.uy; hcerecet@fq.edu.uy

0968-0896/$ - see front matter © 2006 Published by Elsevier Ltd.
doi:10.1016/j.bmc.2006.04.041

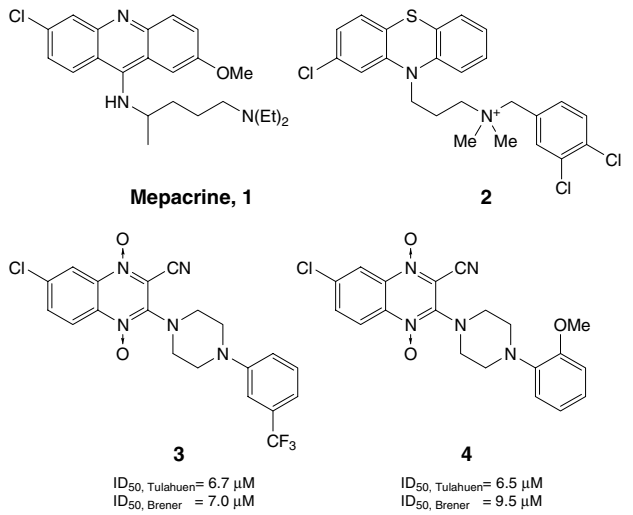

Chart 1. Recognized TR inhibitors and structurally related quinoxaline N^1,N^4-dioxide *Trypanosoma cruzi* growth inhibitors.

selected from our more than 100 quinoxaline library in order to evaluate them against *T. cruzi*. While 3-amino-substituted-2-carbonitrile derivatives (i.e., **3** and **4**, Chart 1) resulted in good in vitro *T. cruzi* growth inhibitors,[15] the 3-amino-2-carbonitrile derivatives were inactive (i.e., **5**–**8**, Chart 2). However, the QSAR study developed predicts derivatives **5**–**8** to be more active than experimentally found, that is, percentage of growth inhibition for derivative **5** at 25 μM would be 60% but experimentally this compound inhibited 25% at this concentration. The low activities displayed by these derivatives could be the result of their low solubilities in the physiological media.[16,17] Another possibility, which was not identified in our previous QSAR studies,[15] is that anti-*T. cruzi* agents must comply with specific structural requirements, that is, volume in the 3-amino moiety like derivatives (**3** and **4**, Chart 1).

In recent papers we have reported the synthesis, characterization, and biological studies of a series of novel vanadyl complexes (**6V**, **7V**, **10V**, and **11V**, Chart 2) with bidentate 3-aminoquinoxaline-2-carbonitrile N^1,N^4-dioxide derivatives as ligands.[18,19] One of the most important physicochemical features of these complexes is their improved solubility in hydrophilic media.

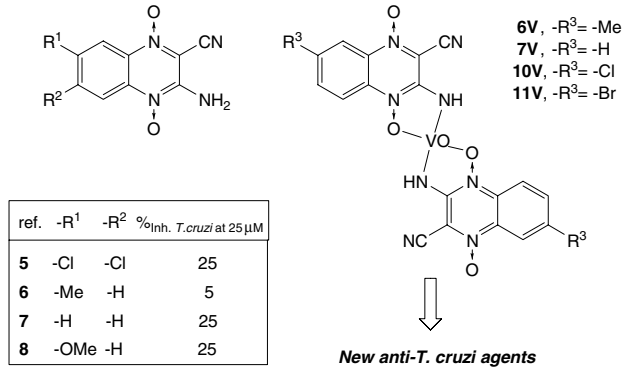

ref.	-R^1	-R^2	%Inh. *T.cruzi* at 25 μM
5	-Cl	-Cl	25
6	-Me	-H	5
7	-H	-H	25
8	-OMe	-H	25

Chart 2. Quinoxaline N^1,N^4-dioxide derivatives, inactive against *Trypanosoma cruzi*, and their vanadyl complexes.

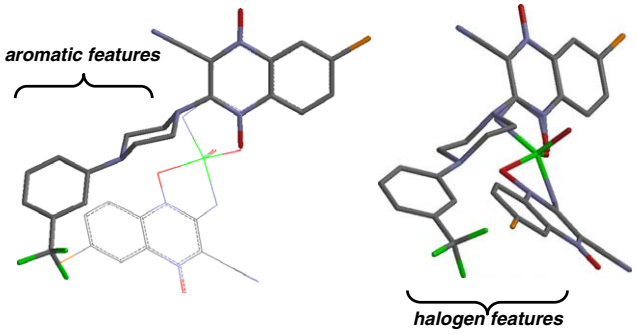

Figure 1. Superimposed minimum-energy conformers of quinoxaline **3** and vanadyl complex **10V**, molecular modeled using semiempirical PM3 (hydrogens were omitted).[28,29] Left: phenyl substituent of **3** (tube) is located in the same spatial region of aromatic system of complex **10V** (wire). Right: stereoview of both compounds (tube) observing the spatial proximity of halogen atoms.

On the other hand, the structure of these products resembles the framework of one of the best quinoxaline anti-*T. cruzi* agents (**3**, Fig. 1). Although the inhibition of *T. cruzi* acidocalcisome, an organelle with specific functions in the parasite homeostasis,[20,21] by vanadate has been recently described,[22] vanadium complexes have not been previously described as anti-*T. cruzi* agents. Medicinal applications of vanadium compounds have mainly focused on their in vitro and in vivo activity in the treatment of diabetes, but tumor growth inhibition and prophylaxis against carcinogenesis due to selected vanadium compounds are well known.[23–27] Having this in mind, we have studied the complexation of 3-amino-2-carbonitrile-quinoxaline N^1,N^4-dioxide derivatives with vanadium as an effort to develop novel anti-*T. cruzi* agents by improving bioavailability of the organic ligands and changing the volume at the 3-amino level.

In this work, three new $V^{(IV)}$ complexes with general formulae $V^{IV}O(L)_2$, with L = 6(7)-substituted-3-aminoquinoxaline-2-carbonitrile N^1,N^4-dioxide, have been synthesized and fully characterized. Characterization results were compared with those previously reported for the analogous vanadium complexes (**6V**, **7V**, **10V**, and **11V**, Chart 2) of this series.[18,19] In addition, the ability of the ligands and their complexes to inhibit *T. cruzi* growth was tested. Complex lipophilicity was determined and R^3-substituent physicochemical properties were studied as anti-parasite descriptors.

2. Methods and results

2.1. Synthesis

Three novel vanadyl complexes $V^{IV}O(L)_2$ (**8V**, **9V**, and **12V**, Scheme 1), with L = 3-amino-6(7)-methoxyquinoxaline-2-carbonitrile N^1,N^4-dioxide and 3-amino-6(7)-fluoroquinoxaline-2-carbonitrile N^1,N^4-dioxide, and 3-amino-6(7)-trifluoromethylquinoxaline-2-carbonitrile N^1,N^4-dioxide were synthesized in good yield and high purity by reaction of 1 equiv of $V^{IV}O(acac)_2$ (where acac = acetylacetonate), **13**, with 2 equiv of the corresponding quinoxaline N^1,N^4-dioxide, **8**, **9** or **12**,

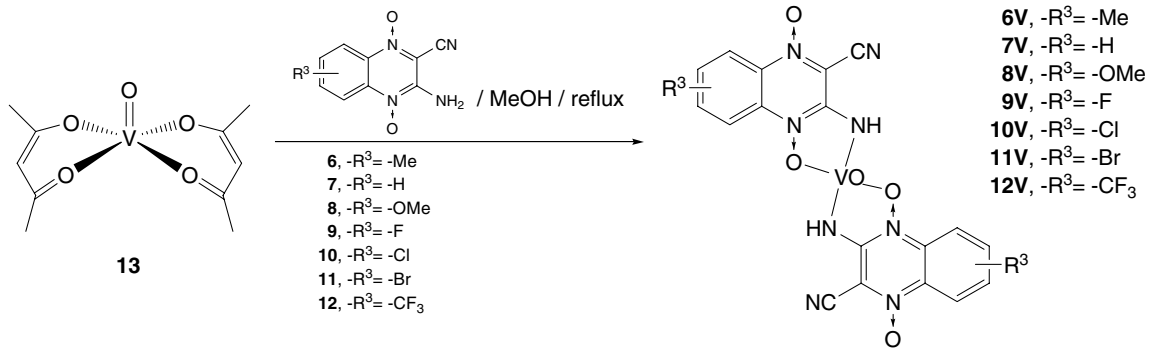

Scheme 1. Synthesis of vanadium complexes **6V**–**12V**.

in methanol under reflux, through a ligand substitution reaction where both acetylacetonates act as leaving groups.[30] Attempts to react quinoxaline N^1,N^4-dioxide **5** with $V^{IV}O(acac)_2$ were unsuccessful due to the very low solubility of the ligand in the solvent of reaction. The *N*-oxide moiety together with the amino group, having suitable donor atoms, coordinates to the vanadium atom. Quinoxaline N^1,N^4-dioxides (**6**–**12**,[12–14,31] Scheme 1) resulted interesting tools for the development of the desired compounds, due to their different electronic and lipophilic properties that could lead to different biological responses. They were prepared with excellent yields from the corresponding benzofuroxan and were generated as a mixture of 6- and 7-substituted isomers that were not possible to separate either by chromatography or by crystallization.[31] Complexes were characterized by microanalysis (C, H, N, and V) conductometric measurements, FAB-MS, and FT-IR spectroscopy (Table 1). Results of the vanadium quantification performed to the new complexes and to the other complexes of the series previously developed are summarized in Table 2. It is interesting to note that the quantification procedure was improved in order to allow the determination of vanadium in vanadyl coloured complexes by performing an acid oxidative process that destroyed organic matter and oxidized vanadyl to vanadate.

Table 2. Results of vanadium determination (V%) for selected derivatives

Compound	V%	
	Calculated	Found[a]
6V	10.2	10.8
7V	10.8	10.2
8V	9.6	9.5
10V	9.4	9.0
11V	8.1	7.9

[a] Mean value of two determinations.

Conductometric measurements performed to 10^{-4}–10^{-3} M DMF solutions of the complexes showed that they behave as nonelectrolytes, in agreement with the assigned formula. FTIR spectra of the new complexes showed a similar pattern to those previously reported for $V^{IV}O(L)_2$ complexes with **6**, **7**, **10**, and **11** as ligands.[18,19] Relevant vibrational bands

Table 1. Selected infrared vibrational bands (cm^{-1}) of the new vanadyl complexes, $VO(L)_2$, in comparison with those previously reported for **6V**, **7V**, **10V**, and **11V**,[18,19] and the free ligands

Compound	Infrared bands						
	$\nu_{as}NH_2$	ν_sNH_2	νN–H	νN–O	νC=N → O	νC≡N	νV=O
6	3329 s	3264 m		1333 vs	1617 s; 1644 s	2233 w	—
6V	—	—	3338 m, br	1340 vw[a]	1555 s; 1616 sh	2230 w	965 s
7	3353 s	3262 s		1343 vs	1604 s; 1626 s	2237 w	—
7V	—	—	3318 m, br	1330 vw[a]	1553 s; 1611 s	2231 w	991 s
8	3338 s	3276 m	—	1336 vs	1617 s; 1645 s	2236 w	—
8V	—	—	3344 m, br	1340 vw[a]	1555 s; 1612 sh	2229 w	984 s
9	3336 s	3255 s	—	1345 vs	1594 s; 1630 s	2231 w	—
9V	—	—	3331 m, br	1339 vw[a]	1555 s; 1619 sh	2234 w	992 s
10	3430 s	3295 s	—	1343 vs	1604 s; 1626 s	2237 w	—
10V	—	—	3334 m, br	1338 vw[a]	1557 s; 1611 s	2229 w	980 s
11	3436 s	3295 s	—	1335 vs	1613 s; 1648 s	2237 w	—
11V	—	—	3346 m, br	1336 vw[a]	1559 s; 1618 sh	2230 w	978 s
12	3403s	3284m	—	1347 vs	1614 s; 1627 s	2226 w	—
12V	—	—	3342 m, br	1340 vw[a]	1578 s; 1629 sh	2232 w	977 s

ν: stretching, ν_{as}: asymmetric stretching, ν_s: symmetric stretching, br: broad, sh: shoulder, s: strong, m: medium, w: weak, vw: very weak.
[a] See text.

are summarized in Table 1. The IR spectra of each of the new complexes showed the typical strong band due to the V=O stretching mode of the VO^{2+} moiety in the region 965–990 cm^{-1}.[32] The strong bands corresponding to $\nu_{as}(NH_2)$ and $\nu_s(NH_2)$ of the amino group, located in the 3200–3450 cm^{-1} region, disappeared and only one band (ν(NH)) of medium intensity around 3300–3350 cm^{-1} was observed, supporting the coordination of the ligand to vanadium through the deprotonated amino group.[18,19,31,33,34] This deprotonation of the aromatic amine group has been previously reported for vanadium (see Table 1)[18,19] and copper complexes of this family of ligands[31] and for metal chelates of quinoline *N*-oxides and other aromatic amine *N*-oxides involving an amine substituent in *ortho* position to the *N*-oxide.[35] The strong $\nu(N \rightarrow O)$ stretching mode, located near 1340 cm^{-1} for the free ligands, turned to weak in the vanadium complex without a significant displacement. As previously reported, this effect could be explained by the coordination of only one of the $N \rightarrow O$ groups per ligand molecule, keeping the other $N \rightarrow O$ group uncoordinated.[18,19] IR spectra showed that the $\nu(C{\equiv}N)$ suffered only minor changes in agreement with the fact that this group was not coordinated to the metal.

The results of the physicochemical characterization performed to the new vanadium complexes and their comparison with those of the four vanadyl compounds previously described are partially summarized in Tables 1 and 2, confirm that the new compounds are analogous. They are neutral vanadyl $V(^{IV})$ complexes with two molecules of deprotonated 3-amino-6(7)-substituted quinoxaline-2-carbonitrile N^1,N^4-dioxide derivative as ligand, coordinated through the amine and the neighboring $N \rightarrow O$ group to the vanadium central atom. On the other hand, of particular biological significance is the fact that the solubility in hydrophilic solvents, like light alcohols, resulted significantly higher for the vanadyl complexes than for the free ligands. The complexes result soluble in acetonitrile, dichloromethane, dimethylsulfoxide (DMSO) and dimethylformamide (DMF) and partially soluble in methanol, ethanol, and water. Despite this favourable solubility behavior it was not possible to attain single crystals adequate for crystallographic studies.

2.2. Biological characterization

2.2.1. Anti-trypanosomal activities. As a first screening the ability of complexes **6V**–**12V** and ligands **9**–**12** to inhibit the growth of the epimastigote form of *T. cruzi* (Tulahuen 2 strain) was evaluated at 25 μM and the IC_{50} was determined for the most active compounds (Table 3).[36–38] Parasites were grown in the presence of the compound for five days and the percentage of growth inhibition (PGI) was determined against control (no drug added to the medium) as explained in experimental section. Nfx and Bnz were used as the reference trypanocidal drug and $V^{IV}O(acac)_2$, **13**, was included to know the trypanocidal effect of vanadium, as vanadyl entity.

Table 3. In vitro anti-*Trypanosoma cruzi* behavior and lipophilic characterization of the developed vanadium compounds and the free ligands

Compound	Biological activity		R_M[c]	–R[3d]	σ_m[e]
	PGI (%)[a,b]	IC_{50}[a,b] (μM)			
6	5.0	nd[f]	−3.5	–Me	−0.7
6V	47.5	27.0	−2.3		
7	25.0	nd	nd	–H	0.0
7V	59.5	20.0	−4.8		
8	25.0	nd	nd	–OMe	1.2
8V	43.5	35.0	−5.2		
9	5.0	nd	nd	–F	3.4
9V	84.0	19.9	−4.3		
10	0.0	nd	nd	–Cl	3.7
10V	95.0	16.8	−2.5		
11	31.5	nd	−1.8	–Br	3.9
11V	91.5	12.8	−1.9		
12	0.0	nd	−1.0	$–CF_3$	4.3
12V	15.5	nd	−0.7		
13	13.5	nd	—	—	—
Nfx	92.0	7.7	—	—	—
Bnz	93.0	8.5	—	—	—

Physicochemical descriptor of quinoxaline ligand R^3-substituents.
[a] PGI: percentage of growth inhibition at 25 μM.
[b] The results are mean values of three different experiments with a SD less than 10% in all cases.
[c] $R_M = \log[(1/R_f) - 1]$. To autoscale this independent variable, the R_M reported are $10\times R_M$, being R_M the values experimentally obtained.
[d] According to Scheme 1.
[e] From Refs. 42,43. To autoscale this independent variable, the σ_m reported are $10 \times \sigma_m$, being σ_m the substituent constants.
[f] nd, not determined.

2.3. Lipophilicity studies

Lipophilicity was experimentally determined in order to study the change of ligands' physicochemical properties due to the complexation to vanadium and their relationship with activity. Reversed-phase TLC experiments were performed for all the derivatives on precoated TLC-C_{18} and eluted with MeOH–physiological serum (40:60, v/v). The R_f values were converted into R_M[39] values via the relationship: $R_M = \log[(1/R_f) - 1]$.[40–42] Table 3 summarizes R_M for each compound.

2.4. Structure–activity relationships

Structure–activity relationship studies were performed in order to know the vanadyl complexes' structural requirements for optimal activity. In this sense, electronic and lipophilic substituent descriptors (Hammett constants, σ_p, σ_m, and σ_I, and π constants)[43,44] and values of R_M were examined in this study. The substituent π constants resulted linearly correlated with the experimental values of R_M ($r = 0.9691$, $p = 0.0003$). In Eq. 1, n represents the number of data points, r is the root of correlation coefficient, s is the standard deviation of the regression equation, the F value is related to the F-statistic analysis (Fischer test), and r^2_{adj} defines the cross-validated correlation coefficient. Only structure–activity models having a value of r^2_{adj} above 0.5 were considered. Activity used in the structure–activity relationship studies was the inhibitory effect on the growth of *T. cruzi* expressed as percentage of growth inhibition at day 5 at

25 μM concentration, PGI. We used $\log_{10}$ (PGI) values as the dependent variables in the linearization procedure. First, one-variable and multivariable regressions between activity and the physicochemical properties were studied. The best one-variable equation was obtained when we analyzed the correlation between $\log_{10}$ (PGI) and R_M ($r = 0.9067$) resulting a typical quadratic correlation (Fig. 2a). In order to analyze the influence of the substituent electronic character on the activitym we included Hammett constants in the studies and the best multivariable correlation was obtained when we analyzed the correlation between $\log_{10}$ (PGI) and the independent variables R_M and σ_m (Eq. 1). Besides, the correlation matrix for the used physicochemical descriptors was performed and cross-correlations between the descriptors used in this equation were not obtained. These parameters are therefore orthogonal, a fact that affords their use in the multilinear regression procedure.[45]

$$\begin{aligned}\log_{10}(\mathrm{PGI}) &= 0.50(\pm 0.21) + 0.05(\pm 0.02)\sigma_m \\ &\quad - 0.82(\pm 0.14)R_M - 0.12(\pm 0.02)R_M^2 \\ r^2 &= 0.9264,\ r^2_{adj} = 0.8527,\ s = 0.1057, \\ F &= 12.58,\ p = 0.033,\ n = 7\end{aligned} \tag{1}$$

3. Discussion

Three new vanadium complexes coordinated to 3-aminoquinoxaline-2-carbonitrile N^1,N^4-dioxide derivatives, **8V**, **9V**, and **12V**, have been successfully developed following an efficient methodology. Their physicochemical behavior, especially solubilities in hydrophilic solvents, showed to be similar to that of the previously described analogues **6V**, **7V**, **10V**. and **11V**. The new anti-*T. cruzi* evaluation of the free ligands, **9**–**12**, confirmed the low activity pattern of this kind of quinoxaline N^1,N^4-dioxide derivatives. The anti-*T. cruzi* activity displayed by vanadium complexes, **6V**–**12V**, resulted in all cases to be better than the activity of each of the corresponding free ligands. The new vanadium complex **9V** and the previously described **10V** and **11V** have shown excellent anti-*T. cruzi* activity with IC_{50} values in the same order of that of Nfx and Bnz.

According to the structure–activity studies, the biological response of this family of complexes depends on the lipophilic properties (Fig. 2a), being the most lipophilic complex, derivative **12V** (see R_M value in Table 3), the least active compound. However, according to Eq. 1 the electronic effect of the quinoxaline substituents plays a role in the complexes anti-parasitic activity. Halogen substituents, F, Cl, and Br, are present in the most active derivatives, compounds **9V**, **10V**, and **11V**, respectively. Eq. 1 indicates that when σ_m increases, the percentage of parasite inhibition increases. Derivative **12V** is an outlier of this rule due to its high hydrophilic character.

The results indicate that the vanadium complexation improves the bioavailability of the bioactive entity, the quinoxaline N^1,N^4-dioxide system. The low bioactivity of precursor **13** and some quinoxaline complexes, that is, derivative **12V**, indicates that vanadyl entity does not posses anti-*T. cruzi* activity per se, behaving in this sense different to vanadate anion.[22]

While we did not fit quinoxaline N^1,N^4-dioxides **6**–**12** in our previous QSAR equation,[15] in the current approach the complexation allows to analyze quinoxaline substituent constants, like σ_m, in a QSAR study. This fact shows that the inadequate physicochemical properties of compounds **6**–**12**, that is, low hydrophilic solvent solubility, affect the biological properties of these derivatives.

4. Conclusions

The results presented above indicate that the developed vanadium complexes could be a good starting point for further chemical modifications in order to improve the anti-*T. cruzi* activity of the selected ligands. The structure–activity relationship obtained in this work provides a guide to design new vanadyl complexes with this family of ligands, which could show the desired activity. Synthetic attempts in this direction are currently in progress.

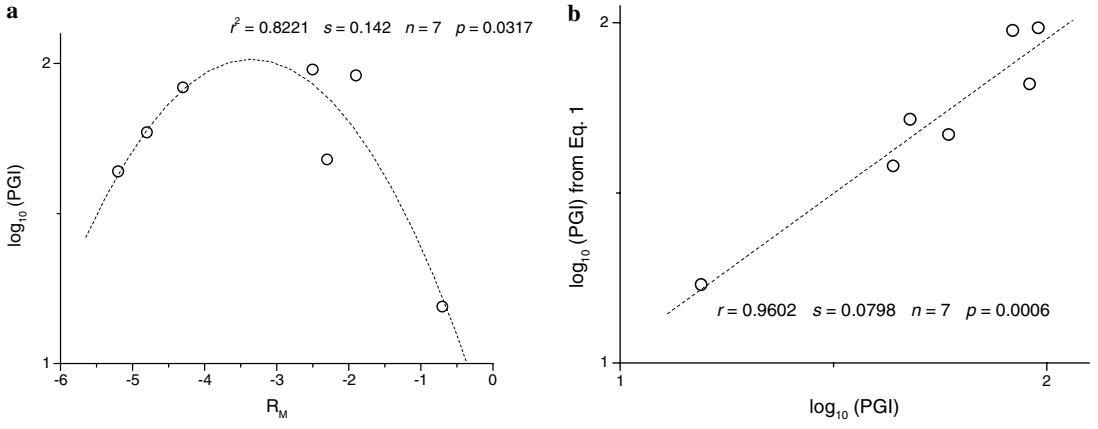

Figure 2. (a) R_M versus $\log_{10}$ of percentage of trypanosome growth inhibition at 25 μM ($\log_{10}$ (PGI)). (b) Plot of $\log_{10}$ (PGI) experimental versus calculated values from Eq. 1.

5. Experimental

5.1. Chemistry

All common laboratory chemicals were purchased from commercial sources and used without further purification. The ligands **5**–**12** were synthesized as a mixture of 6- and 7-substituted isomers by reaction of the corresponding benzofuroxan and malonitrile, and characterized, as previously described.[12] $V^{IV}O(acac)_2$, **13**, was prepared according to a well-established literature procedure.[30] The complexes **6V**, **7V**, **10V**, and **11V** were prepared as previously described.[18,19] For the organic procedures the solvents were dried and distilled prior to use, and the reactions were carried out in a nitrogen atmosphere. C, H, and N analyses were performed with a Carlo Erba Model EA1108 elemental analyzer. Vanadium was determined by a modification of the tungstophosphate method.[46] Previously, destruction of organic matter was performed by boiling the sample with sulfuric acid–nitric acid. In the process vanadium(IV) is oxidized to vanadate which is determined spectrophotometrically after addition of phosphoric acid and sodium tungstate. Routine FAB+ spectra of the metal complexes were measured up to *m*/*z* = 1500 with a TSQ spectrometer (Finnigan) with nitrobenzylalcohol as matrix. The ion gun was operated at 8 kV and 100 μA (probe temperature: 50 °C). Xenon was used as primary beam gas. Conductometric measurements were performed at 25 °C in 10^{-3} M dimethylformamide solutions using a Conductivity Meter 4310 Jenway.[47] FTIR spectra (4000–400 cm^{-1}) were measured as KBr pellets on a Bomen M102 instrument.

5.1.1. General procedure for the synthesis of vanadium complexes (8V, 9V, and 12V). A mixture of $V^{IV}O(acac)_2$ (**13**, 60 mg, 0.227 mmol), the corresponding ligand (**8** or **9**, 0.454 mmol), and methanol (18 mL) as solvent was heated at reflux during 24–30 h. The vanadyl complexes were filtered off from the hot solution as red solids. For the synthesis of derivative **12V** 10 mL of methanol was used, the reflux was maintained during 36 h, and the product was separated as a red solid by partial evaporation of the methanolic solution.

5.1.1.1. [$V^{IV}O$(3-amino-6(7)-methoxyquinoxaline-2-carbonitrile N^1,N^4-dioxide)$_2$] (8V). Yield 23 mg (55%). Anal. Calcd for $VO(C_{10}H_7N_4O_3)_2{\cdot}3H_2O$: C, 41.18; H, 3.46; N, 19.21. Found: C, 41.89; H, 3.34; N, 19.30. FAB+ MS *m*/*z* (assignment, percentage): 530 ($M^{+\cdot}$+H$^{\cdot}$, 61%), 513 ($M^{+\cdot}$−O$^{\cdot}$, 59%), 502 ($M^{+\cdot}$−HCN$^{\cdot}$, 8%), 307 ($C_9H_{12}N_4O_5V^{+\cdot}$, 100%), 289 ($C_9H_{10}N_4O_4V^{+\cdot}$, 60%) and 233 (L+H$^{\cdot}$, 20%).

5.1.1.2. [$V^{IV}O$(3-amino-6(7)-fluoroquinoxaline-2-carbonitrile N^1,N^4-dioxide)$_2$] (9V). Yield 34 mg (59%). Anal. Calcd for $VO(C_9H_4N_4O_2F)_2{\cdot}H_2O$: C, 41.32; H, 1.93; N, 21.41. Found: C, 42.52; H, 2.06; N, 21.79. FAB+MS *m*/*z* (assignment, percentage): 495 ($VO(C_9H_4N_4O_2F)_2{\cdot}$ H$_2$O−HCN$^{\cdot}$, 4%), 402 ($C_{17}H_{10}FN_5O_3V^{+\cdot}$, 10%), 374 ($C_{16}H_{13}N_5O_3V^{+\cdot}$, 4%) and 202 (L+H$^{\cdot}$−F$^{\cdot}$, 100%).

5.1.1.3. [$V^{IV}O$(3-amino-6(7)-trifluoromethylquinoxaline-2-carbonitrile N^1,N^4-dioxide)$_2$] (12V). Yield 23 mg (41%). Anal. Calcd for $VO(C_{10}H_4F_3N_4O_2)_2{\cdot}H_2O$: C, 38.54; H, 1.62; N, 17.91. Found: C, 39.02; H, 1.55; N, 17.90. FAB+MS *m*/*z* (assignment, percentage): 605 ($M^{+\cdot}$, 40%), 589 ($M^{+\cdot}$−O$^{\cdot}$, 20%), 580 ($M^{+\cdot}$−CN$^{\cdot}$+H$^{\cdot}$, 5%), 336 ($M^{+\cdot}$−L$^{\cdot}$, 35%) and 271 (L+H$^{\cdot}$, 100%).

5.2. Biology

5.2.1. Trypanocidal in vitro test. *Trypanosoma cruzi* epimastigotes (Tulahuen 2 strain) were grown at 28 °C in an axenic medium (BHI-tryptose) as previously described, complemented with 5% fetal bovine serum. Cells from a 10-day-old culture (stationary phase) were inoculated into 50 mL of fresh culture medium to give an initial concentration of 1×10^6 cells/mL. Cell growth was followed by measuring everyday the absorbance of the culture at 600 nm. Before inoculation, the media were added to the indicated amount of the drug from a stock solution in DMSO. The final concentration of DMSO in the culture media never exceeded 0.4% and the control was run in the presence of 0.4% DMSO and in the absence of any drug. No effect on epimastigote growth was observed by the presence of up to 1% DMSO in the culture media. The percentage of inhibition was calculated as follows: $\% = \{1-[(A_p - A_{0p})/(A_c - A_{0c})]\} \times 100$, where $A_p = A_{600}$ of the culture containing the drug at day 5; $A_{0p} = A_{600}$ of the culture containing the drug just after addition of the inocula (day 0); $A_c = A_{600}$ of the culture in the absence of any drug (control) at day 5; $A_{0c} = A_{600}$ in the absence of the drug at day 0.

5.3. Lipophilicity studies

Reversed-phase TLC experiments were performed on precoated TLC plates SIL RP-18 W/UV_{254} and eluted with MeOH–physiological serum (40:60, v/v). Stock solutions were prepared in pure acetone (Aldrich) prior to use. The plates were developed in a closed chromatographic tank, dried and the spots were located under UV light. The R_f values were averaged from two to three determinations and converted into R_M.

Acknowledgments

This work was supported by CHLCC-Uruguay (Projects CHLCC2002/43, CHLCCFMP20042), CSIC (Project 293/04), and PEDECIBA of Uruguay and collaborative program CYTED. We thank Prof. Dr. Ulrich Abram (Institut für Chemie, Anorganische und Analytische Chemie, Freie Universität Berlin) for performing the FAB-MS experiments.

References and notes

1. World Health Organization: http://www.who.int/ctd/chagas.
2. Moncayo, A. In *WHO Special Program for Research and Training in Tropical Diseases (TDR)*; World Health Organization Ed., Eleventh Programme Report of the UNPD: World Bank: Geneva, 1993; pp 67–75.

3. De Souza, W.. *Curr. Pharm. Des.* **2002**, *4*, 269.
4. Cerecetto, H.; González, M. *Curr. Top. Med. Chem.* **2002**, *2*, 1187.
5. Castro, J. A.; Díaz de Toranzo, E. G. *Biomed. Environ. Sci.* **1988**, *1*, 19.
6. Gorla, N. B.; Ledesma, O. S.; Barbieri, G. P.; Larripa, I. B. *Mutat. Res.* **1989**, *224*, 263.
7. Croft, S. L. *Mem. Inst. Oswaldo Cruz* **1999**, *94*, 215.
8. Schmidt, A.; Krauth-Siegel, R. L. *Curr. Top. Med. Chem.* **2002**, *2*, 1239.
9. Jacoby, E. M.; Schlichting, I.; Lantwin, C. B.; Kabsch, W.; Krauth-Siegel, R. L. *Proteins* **1996**, *24*, 73.
10. Krauth-Siegel, R. L.; Lohrer, H.; Bücheler, U. S.; Schirmer, R. H. In *Biochemical Protozoology*; Coombs, G., North, M., Eds.; Taylor and Francis: London, 1991; pp 493–506.
11. Khan, M. O.; Austin, S. E.; Chan, C.; Yin, H.; Marks, D.; Vaghjiani, S. N.; Kendrich, H.; Yardley, V.; Croft, S. L.; Douglas, K. T. *J. Med. Chem.* **2000**, *43*, 3148.
12. Monge, A.; Martínez-Crespo, F. J.; López de Ceráin, A.; Palop, J. A.; Narro, S.; Senador, V.; Marín, A.; Sáinz, Y.; González, M.; Hamilton, E.; Barrer, A. J. *J. Med. Chem.* **1995**, *38*, 4488.
13. Ortega, M. A.; Morancho, M. J.; Martínez-Crespo, F. J.; Sáinz, Y.; Montoya, M. E.; López de Ceráin, A.; Monge, A. *Eur. J. Med. Chem.* **2000**, *35*, 21.
14. Zarranz, B.; Jaso, A.; Aldana, I.; Monge, A. *Bioorg. Med. Chem.* **2004**, *12*, 3711.
15. Aguirre, G.; Cerecetto, H.; Di Maio, R.; González, M.; Montoya Alfaro, M. E.; Jaso, A.; Zarranz, B.; Ortega, M. A.; Aldana, I.; Monge, A. *Bioorg. Med. Chem. Lett.* **2004**, *14*, 3835.
16. Zamalloa, E.; Aldana, I.; Bachiller, C. M.; Monge, A. *Arzneim.-Forsch.* **1997**, *47*, 873.
17. Zamalloa, E.; Dios-Viéitez, C.; González-Peña, E.; Monge, A. *Arzneim.-Forsch.* **1997**, *47*, 1044.
18. Noblía, P.; Vieites, M.; Torre, M. H.; Costa-Filho, A. J.; Cerecetto, H.; González, M.; Lavaggi, M. L.; Adachi, Y.; Sakurai, H.; Gambino, D. *J. Inorg. Biochem.* **2006**, *100*, 281.
19. Vieites, M.; Noblía, P.; Torre, M. H.; Cerecetto, H.; Lavaggi, M. L.; Costa Filho, A. J.; Azqueta, A.; López de Cerain, A.; Monge, A.; Parajón-Costa, B.; González, M.; Gambino, D. *J. Inorg. Biochem.*, in press, doi:10.1016/j.jinorgbio.2006.03.012.
20. Docampo, R.; Scott, D. A.; Vercesi, A. E.; Moreno, S. N. *Biochem. J.* **1995**, *310*, 1005.
21. Urbina, J. A.; Moreno, B.; Vierkotter, S.; Oldfield, E.; Payares, G.; Sanoja, C.; Bailey, B. N.; Yan, W.; Scott, D. A.; Moreno, S. N. J.; Docampo, R. *J. Biol. Chem.* **1999**, *274*, 33609.
22. Docampo, R.; Moreno, S. N. J. *Mol. Biochem. Parasitol.* **2001**, *33*, 151.
23. Baran, E. J. *J. Inorg. Biochem.* **2000**, *80*, 1.
24. Orvig, C.; Thompson, K. H.; Battell, M.; McNeill, J. H. In Sigel, H., Sigel, A., Eds.; Metal Ions in Biological Systems; Marcel Dekker: New York, 1995; Vol. 31, pp 575–594.
25. Rehder, D. *Angew. Chem., Int. Ed. Engl.* **1991**, *30*, 148.
26. Rehder, D. *Coord. Chem. Rev.* **1999**, *182*, 297.
27. Rehder, D. *Inorg. Chem. Commun.* **2003**, *6*, 604.
28. Spartan'04; Wavefunction, Inc. 18401 Von Karman Avenue, Suite 370. Irvine, CA 92612, USA.
29. Hehre, W. J. In *A Guide to Molecular Mechanics and Quantum Chemical Calculations*; Wavefunction Inc. CA, 2003.
30. Morley, C. P. In *Inorganic Experiments*; Derek, J. W., Ed.; VCH: Weinheim, 1994; pp 113–114.
31. Torre, M. H.; Gambino, D.; Araujo, J.; Cerecetto, H.; González, M.; Lavaggi, M. L.; Azqueta, A.; López de Cerain, A.; Monge-Vega, A.; Abram, U.; da Costa-Filho, A. J. *Eur. J. Med. Chem.* **2005**, *40*, 473.
32. Baran, E. J. *J. Coord. Chem.* **2001**, *54*, 215.
33. Conley, R. T.; Calderón Martínez, J.; Avendaño Ruíz, R. In *Espectroscopía Infrarroja*; Alhambra: Madrid, 1979.
34. Lin-Vien, D.; Colthup, N. B.; Fateley, W. G.; Grasselli, J. G. In *The Handbook of Infrared and Raman Characteristic Frequencies of Organic Molecules*; Academic Press: Boston, 1999.
35. Karayannis, N. M.; Pytlewski, L. L.; Mikulski, C. M. *Coord. Chem. Rev.* **1973**, *11*, 93.
36. Denicola, A.; Rubbo, H.; Rodríguez, D.; Radi, R. *Arch. Biochem. Biophys.* **1993**, *304*, 279.
37. Aguirre, G.; Cerecetto, H.; González, M.; Gambino, D.; Otero, L.; Olea-Azar, C.; Rigol, C.; Denicola, A. *Bioorg. Med. Chem.* **2004**, *12*, 4885.
38. Aguirre, G.; Boiani, M.; Cabrera, E.; Cerecetto, H.; Di Maio, R.; González, M.; Denicola, A.; Sant'Anna, C. M. R.; Barreiro, E. J. *Eur. J. Med. Chem.* **2006**, *41*, 457.
39. Hansch, C.; Leo, A. The Hydrophobic Parameter: Measurement and Calculation. In *Exploring QSAR. Fundamentals and Applications in Chemistry and Biology*; American Chemical Society Ed.: Washington, 1995; pp 97–124.
40. Tsantili-Kakoulidou, A.; Antoniadou-Vyza, A. *Prog. Clin. Biol. Res.* **1989**, *291*, 71.
41. Denny, W. A.; Graham, J. A.; Roberts, P. B.; Anderson, R. F.; Boyd, M.; Lock, C. J. L.; Wilson, W. R. *J. Med. Chem.* **1992**, *35*, 4832.
42. Cerecetto, H.; Di Maio, R.; González, M.; Risso, M.; Saenz, P.; Seoane, G.; Denicola, A.; Peluffo, G.; Quijano, C.; Olea-Azar, C. *J. Med. Chem.* **1999**, *42*, 1941.
43. Hansch, C.; Leo, A. In *Substituent Constants for Correlation Analysis in Chemistry and Biology*; Wiley: New York, 1979.
44. Ruff, F.; Csizmadia, I. G. In *Organic Reactions. Equilibria, Kinetics and Mechanism*; Elsevier: Amsterdam, 1994.
45. Myers, R. H. In *Classical and Modern Regression with Application*; P.W.S. Publishers: Boston, 1986.
46. Onishi, H. Photometric determination of traces of metals. In Winefordner, J. D., Kolthoff, I. M., Eds., 4th ed.; Chemical Analysis. Part IIB: Individual Metals, Magnesium to Zirconium; John Wiley and Sons, 1998; Vol 3.
47. Geary, W. J. *Coord. Chem. Rev.* **1971**, *7*, 81.